Board Level Solder Joint Reliability Assessment Study of Megtron 6 Vs FR-4 Under Power Cycling and Thermal Cycling

By

JYOTIRMOY DENRIA

Presented to the Faculty of the Graduate School of

University of Texas at Arlington in Partial Fulfillment

of the Requirements

For the Degree of

MASTER OF SCIENCE IN MECHANICAL ENGINEERING

THE UNIVERSITY OF TEXAS AT ARLINGTON

December 2017

Acknowledgements

I would like thank Dr. Dereje Agonafer for his immense support and continuous guidance in my master's study and research. His enthusiasm and motivation also pushed me further in this project. A special thanks to him for giving me an opportunity to be a part of the EMNSPC team. I would like thank Dr. A. Haji-Sheikh and Dr. Fahad Mirza for being a part of my thesis committee.

I would like to thank my entire EMNSPC team member. Special thanks to Pawan, Unique, Mugdha, Paul, Mahesh and Abel for their continuous guidance and motivation. A special thanks to Ms. Kathleen, Ms. Wendy, Ms. Flora for assisting me through my degree program.

I am also thankful to my family, friends and my fiancé for nonstop support, care and love. Thank you all for always being there for me.

December 1st, 2017

Abstract

Solder Joint Reliability Assessment Study of Megtron 6 Under Power Cycling and Thermal Cycling

JYOTIRMOY DENRIA, MS
The University of Texas at Arlington, 2017

Supervising Professor: Dereje Agonafer

High frequency laminates like Nelco N4000-13, Isola FR408 and Panasonic Megtron 6 packages gained popularity among the industry due to better and improved electrical performances, Improved impedance control, low moisture absorption, good thermal management. High speed laminates are extensively used in high-speed system-level interconnects like high speed network equipment, mainframes, IC testers and high frequency measuring instruments. When an electronic device is turned off and then turned on multiple times, it creates a loading condition called power cycling. The die is the only heat source causing non-uniform temperature distribution. In this paper, the solder joint reliability assessment of Megtron 6 boards are done using Finite element analysis (FEA) under two different loads power cycling and thermal cycling which act as a combined load. The reliability assessment is done to check stress distribution on PCB boards and solder joint. The life to failure is determined for Megtron 6 board package assembly. The mismatch in coefficient of thermal expansion (CTE) between components used in Megtron 6 and the non-uniform temperature distribution makes the package deform. Modeling of life prediction is usually conducted for Accelerated Thermal Cycling (ATC) condition, which assumes uniform temperature throughout the assembly. An assembly is also subjected to Power Cycling i.e. non-uniform temperature with the chip as the only source of heat generation. This analysis shows the performance of Megtron 6 series vs FR-4 assembly under thermal and power cycle in combination and the stress distribution and plastic work for the package.

In this work, we have used Megtron 6 and Fr-4 circuit boards with BGA packages. Dynamic Mechanical Analyzer (DMA) is used to obtain the time and temperature dependent viscoelastic properties of the boards and Thermo Mechanical Analyzer(TMA) is used to calculate the Co-efficient of Thermal Expansion(CTE) from the boards. The obtained results from the material characterization are used to simulate the Finite Element Analysis (FEA) model. ANSYS Workbench 18 is leveraged to study the life to failure under a combined thermal and power cycling. Plastic work for the boards were also calculated for all the boards and followed by number of cycles to failure which is the most signification concern in the reliability of a package assembly.

Tables of Contents

List of Illustrations

List of Tables

Chapter 1

INTRODUCTION

1.1 Electronic Packaging

Electronic packaging is a major discipline within the field of electronic engineering, and includes a wide variety of technologies. It refers to enclosures and protective features built into the product itself, and not to shipping containers. It applies both to end products and to components. Packaging of an electronic system must consider protection from mechanical damage, cooling, radio frequency emission, protection from electrostatic discharge, maintenance, operator convenience, and cost. Prototypes and industrial equipment made in small quantities may use standardized commercially available enclosures such as card cages or prefabricated boxes. Mass-market consumer devices may have highly specialized packaging to increase consumer appeal. The same electronic system may be packaged as a portable device or adapted for fixed mounting in an instrument rack or permanent installation. Packaging for aerospace, marine, or military systems imposes different types of design criteria. According to the Moore's law, Integrated circuits are getting smaller and complex day by day which makes it difficult to protect them. The numbers of interconnections are increasing with the increase in transistor density coming from the chip to the substrate. Electronic packaging and materials used for printed circuit boards (PCB) and packages have to evolve with increasing use
of high frequency high speed devices with enhanced capabilities.

1.2 High Frequency Laminates

High frequency laminates ensure better and improved electrical performance. Improved impedance control, low moisture absorption and good thermal management than any conventional boards. From he literature, it is very conspicuous that high frequency laminates perform consistently in thermally dynamic environment [3]. High frequency laminates show much better performance than FR4. Reliability, fabrication, performance, material properties are few issues that can be faced while using high frequency laminates. High speed, high frequency laminates like Nelco N4000-13, Isola FR408, and Panasonic Megtron 6 have low dielectric constant (Dk) and low loss tangent [9].

1.3 Moore’s Law

Moore's law is the observation that the number of transistors in a dense integrated circuit doubles approximately every two years. The observation is named after Gordon Moore, the co-founder of Fairchild Semiconductor and Intel, whose 1965 paper described a doubling every year in the number of components per integrated circuit, and projected this rate of growth would continue for at least another decade. Moore's prediction proved accurate for several decades, and has been used in the semiconductor industry to guide long-term planning and to set targets for research and developments.

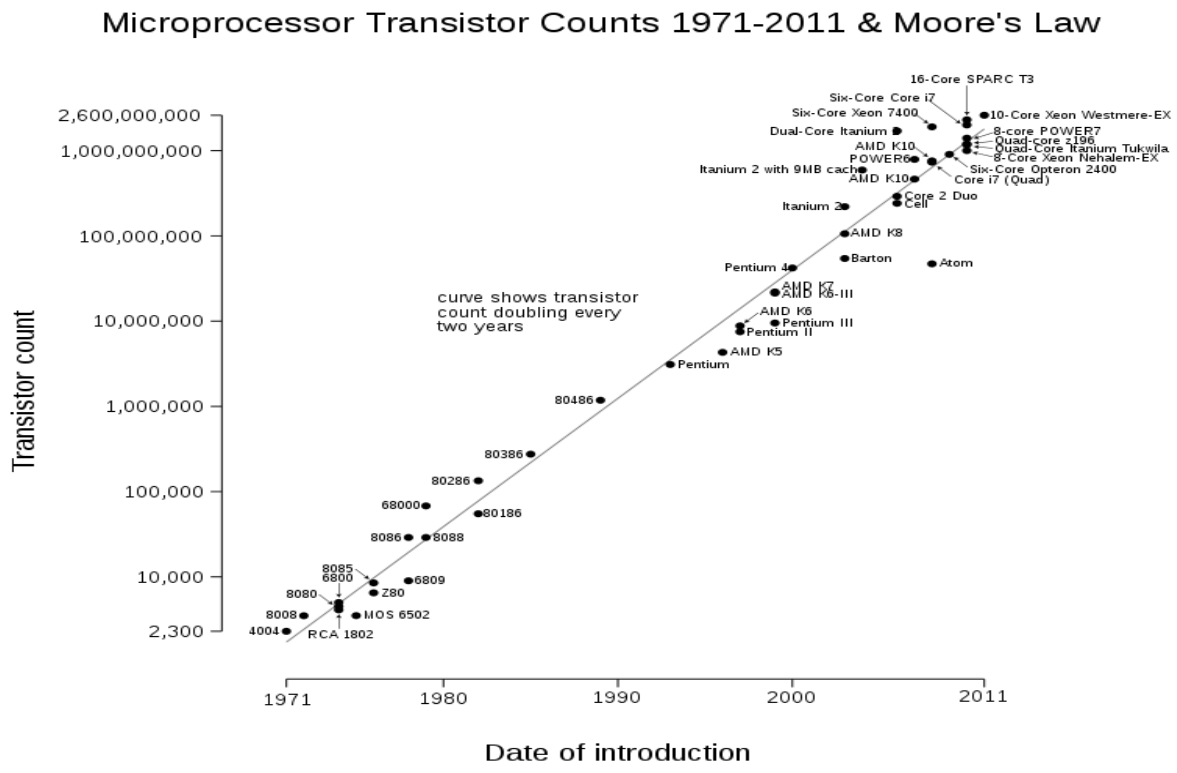

Figure 1.2: Moore’s graph

1.7 Integrated Circuits

Integrated circuits are also known as monolithic integrated circuit which comprises of a set of electronic circuit on one small flat chip or plate of semiconductor material (Silicon). Integrated circuits are usually everywhere as an oscillator, microprocessor, amplifier and many more. With decreasing size of computer, cell phones, electronics the size of the chips or integrated circuits are also reducing. The cost for integrated circuits is reducing too.

There are different types of integrated circuit packages depending on how they are mounted such as surface mount integrated circuit package, through hole mount integrated circuit package and contactless mount integrated circuit package. The following figure shows a tree chart of different types of integrated circuit packaging techniques used.

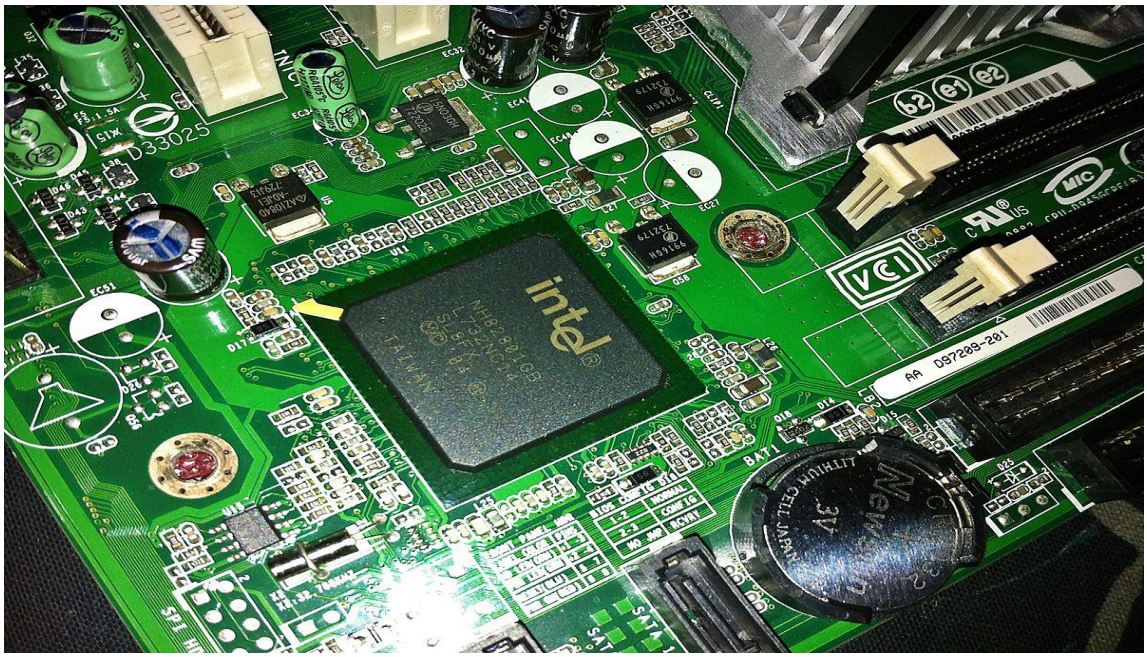

Figure 1.2 Condensed IC package

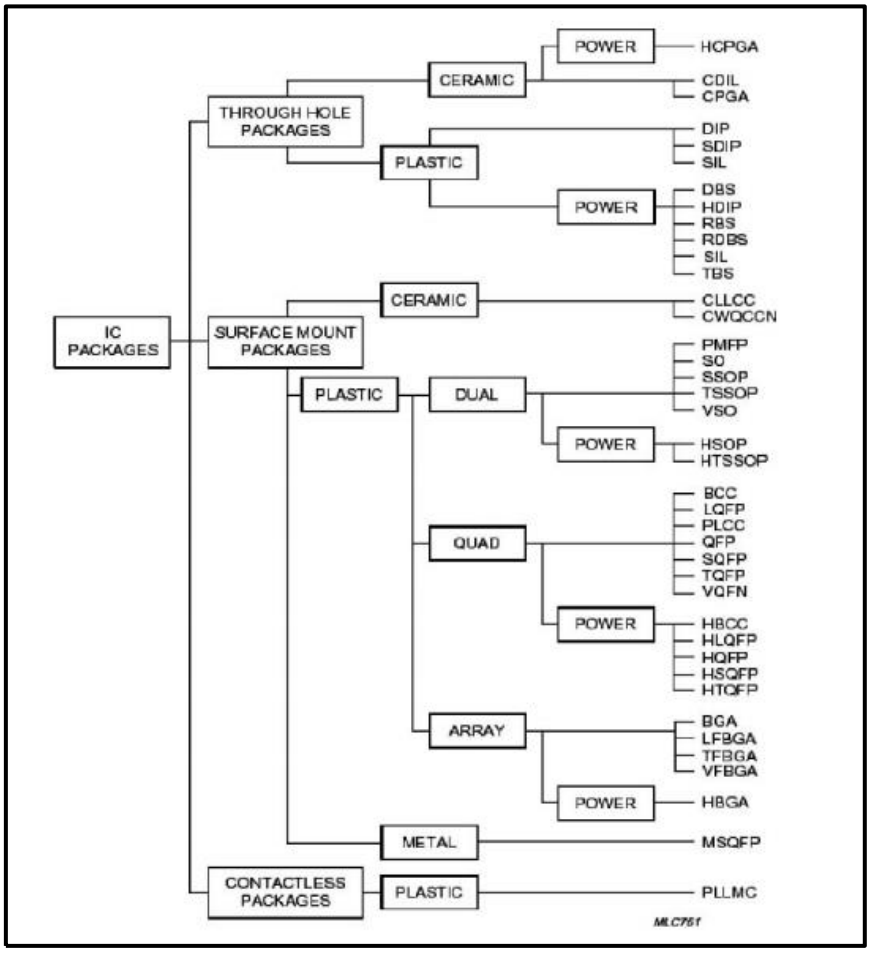

Figure 1.3: Different Types of IC Packaging Techniques

1.5 Ball Grid Array (BGA) Package

BGA is a surface mount technology package used to permanently mount devices such as microprocessors. This package provides more interconnection pins that can be put on a dual in-line or flat package. Complete bottom surface of BGA package is available for interconnections. BGA package has shorter leads and better performance at high speed. This package with a large number of interconnects have a robust design. The underside of this package is used for connections instead of the perimeter unlike the QFN package. In a BGA package the solder balls or bumps

perimeter unlike the QFN package. In a BGA package the solder balls or bumps are placed in a grid, hence the name Ball Grid Array Package, for connectivity on the bottom 4 side of the package or carrier chip BGA has lower thermal resistance as compared to that of the QFN package.

Types of BGA package are as follows:

- *CABGA*: Chip Array Ball Grid Array
- *CTBGA*: Thin Chip Array Ball Grid Array
- *DSBGA*: Die-Size Ball Grid Array
- Fine Ball Grid Array
- *FCmBGA*: Flip Chip Molded Ball Grid Array
- Micro Ball Grid Array
- Plastic Ball Grid Array
- *TABGA*: Tape Array BGA
- *TBGA*: Thin BGA
- *TEPBGA*: Thermally Enhanced Plastic Ball Grid Array
- *VFBGA*: Very Fine Pitch Ball Grid Array

Fig: 1.4 Intel Mobile Celeron in BGA2 Package (FCBGA-479); the die is the blue

Motivations and Objective

Solder joint failure is a major concern in electronic manufacturing companies from a long time. Accelerated Thermal Cycle(ATC) which forces a uniform temperature distribution is most commonly used for solder joint assessment. However, in practical conditions the assembly is subjected to power cycles(PC) which create a non-uniform temperature distribution near the solder joints as die is the only source of heat generation. The mismatch in CTE between components results in deformation of the package. The deformation is different when the package is subjected to ATC only.

The main objective of this study was to analyze the solder joint reliability in BGA packages when power cycling and thermal cycling applied in combined. To understand the root cause of the failure in joints and method to improve the mechanical reliability of the package. In this work we have compared the solder joint reliability of Megtron 6 and FR4 using BGA package. Finding the critical solder joint and obtaining the plastic work followed by the life to failure for that critical solder has been done. We have also compared the performance of Megtron GX, Megtron 4, Megtron 4s, Megtron 2 & Megtron 7.

Chapter 2

LITERATURE REVIEW

S. B. park [3] in his paper has done an accurate assessment of interconnect fatigue life through power cycling. A comparative study was done to predict the life to failure of the BGA package. In this work, the main cause behind the solder joint failure was analyzed and a reliable design was obtained.

John Coonrod [1], has discussed about the use of FR4 and high frequency laminates. The author has basically compared basic material properties, circuit fabrication issues, reliability issues, general end-use consideration, electrical performance consideration and hybrid multilayer PCB for FR4 and high frequency materials. In this article, the author has provided few guidelines to understand when to use a high frequency material and when to use FR4. A discussion on hybrid boards is also done where a combination of FR4 and high frequency laminate is used.

Unique Rahangdale [1] in his paper has done a comparative study of RCC and FR4 BOARDS. The reliability of these boards was characterized in this paper using different machines and results were used for finite element analysis. Directional deformation, equivalent stresses and strains, change in plastic work was obtained from computational analysis using ANSYS. In this paper, advantages of both RCC and FR4 boards were stated. Depending on the demand the two boards can be used as stated in this paper.

Chapter 3

MATERIAL CHARACTERIZATION

It is crucial to acquire accurate material properties of a board for Finite Element Analysis. Coefficient of Thermal Expansion (CTE), Young's Modulus, Storage Modulus (E') and Loss Modulus (E") are obtained through material characterization. We use the Thermo Mechanical Analyzer (TMA) to obtain the CTE value while Young's Modulus, Storage Modulus and Loss Modulus are obtained using Dynamic Mechanical Analyzer (DMA).

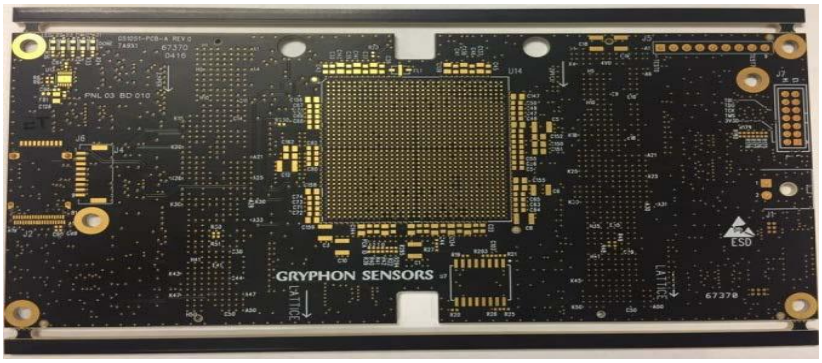

Figure 3.1: Front view of Megtron 6 board

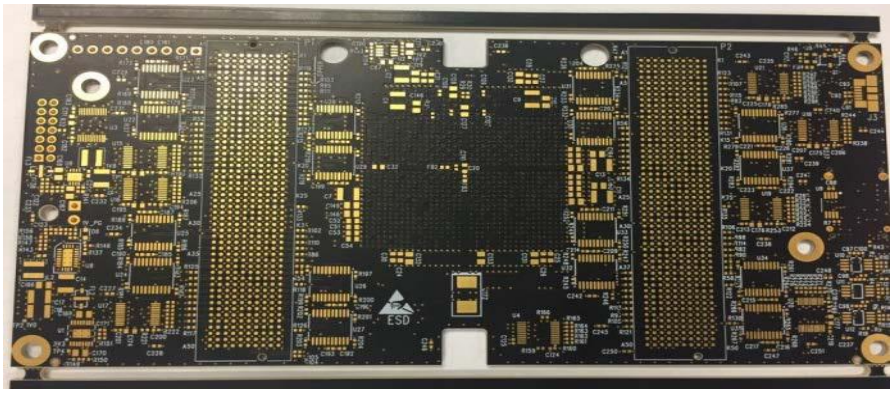

Figure 3.2: Back view of Megtron 6 board

3.1 THERMAL MECHANICAL ANALYZER (TMA)

3.1.1 Coefficient of Thermal Expansion (CTE):

The rate by which a PCB material expands due to heat is called the Coefficient of Thermal Expansion (CTE). CTE can also be defined as the fractional change in length per degree of temperature change

$$\alpha = \frac{\epsilon}{\Delta T}$$

Where,

α – Coefficient of Thermal Expansion (CTE)

$\boldsymbol{\epsilon}$- Strain (mm/mm)

ΔT - Difference in Temperature (^{0}C)

3.1.2 Glass Transition Temperature (Tg):

At this temperature range the polymer chains become more mobile and the PCB substrate transitions from a glassy rigid state to a softened deformable state. The properties are regained once the material cools back to room temperature.

3.1.3 Decomposition Temperature (Td):

At this temperature the PCB material chemically decomposes and it can never regain its original properties upon cooling. It is said that the material losses up to 5% of its mass.

Thermo Mechanical Analyzer (TMA)

TMA is used to measure the In-plane and Out-plane Co-efficient of Thermal Expansion(CTE), Glass Transition Temperature(Tg) and Decomposition Temperature(Td). Temperature range was -65°C to 260°C with a temperature ramp of 5 C°/min. Sample size for TMA experiments were 6 x 6 mm. Samples were made using a high speed cutter. The dimensions of the sample are such that it fits correctly under the probe. The Quartz probe of the TMA sets on the sample and the CTE is obtained from the relative movement of the probe.

Fig :3.3Thermo Mechanical Analyzer (TMA)

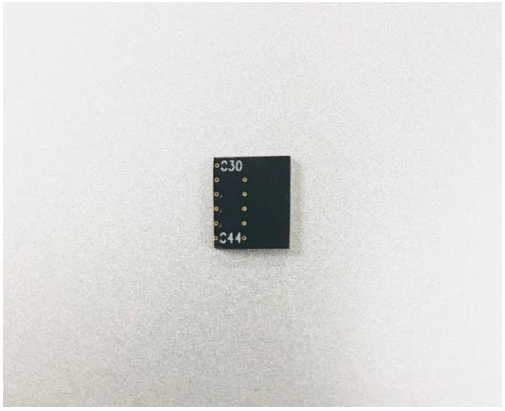

Fig :3.4 Samples used for TMA experiments

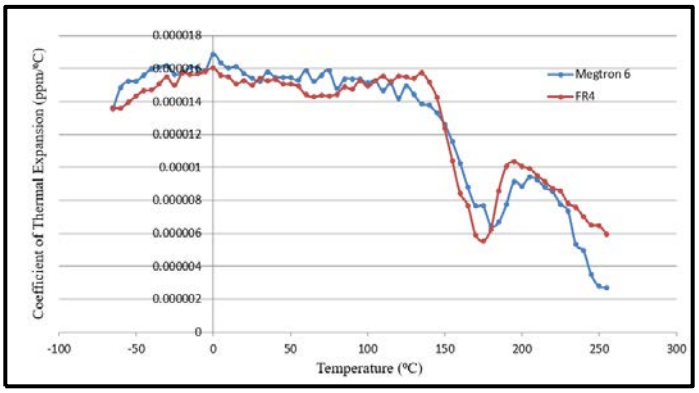

Figure 3.5: Plot for in-plane CTE

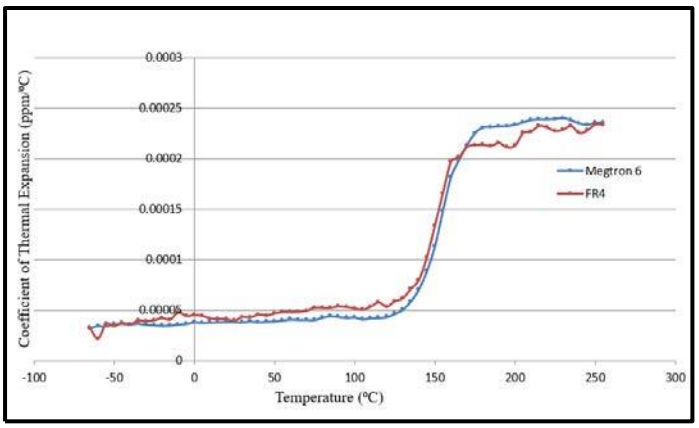

Figure 3.6: Plot for out of plane CTE

The in-plane and out of plane CTE are measured using TMA. Figure 3.5 shows plot for in-plane CTE while figure 3.6 shows plot for out of plane CTE. These coefficients of thermal expansion can be measured by keeping the board sample in three different positions under the quartz probe. A wide variety of thermal loads can be calculated by using a temperature range from -65^{0}C to 260^{0}C. A significant dip can be observed in the in-plane CTE plot after 150^{0}C. This is due to recrystallization and cold crystallization processes occurring in the sample during experiments. Further expansion of sample can be observed above 180^{0}C which at the end melts. The melting process can be seen after about 225^{0}C with decrease in the sample height and viscosity.

Table 3.1 shows the package material properties used in this work. Poisson's ratio for the Megtron 6 board is 0.2 while that for FR4 is 0.39 [11]. Table 3.2 shows all the required material properties used in this study.

Material	CTE (ppm/^{0}C)	E (GPa)
Copper Pad	17.78	110
Die Attach	65	154
Die	2.94	150
Mold	8.43	24
Polyimide Layer	35	3.3
Solder Mask	30	4.6

Table 3.1: Material properties for a BGA package

Boards	CTE (ppm/^{0}C)			E(GPa)
	X direction	Y direction	Z direction	
FR4	15.3	13.1	41.1	15.46
Megtron 6	15.39	13.2	43.1	13.8

Table 3.2: Material Properties of Megtron 6 and FR4 boards

3.2 DYNAMIC MECHANICAL ANALYZER (DMA)

DMA is testing machine which helps us to obtain Young's Modulus(E), Storage Modulus(E') and Loss Modulus(E"). A small sinusoidal load generated by a force motor is applied to sample through a drive shaft. The sample dimensions are kept 10 x 50 mm.

Dynamic Mechanical Analyzer (DMA)

3.2.1 Young's Modulus (E): Young's Modulus is also known as Tensile Modulus or Modulus of Elasticity. It basically measures the stiffness of a PCB. Young's Modulus can be defined as the ration of stress to strain in a particular direction. Materials that deform less as compared to other under tensile loading are said to be stiffer.

3.2.2 Storage Modulus (E'): Storage Modulus measures the stored energy representing elastic portion of a material.

3.2.3 Loss Modulus (E''): Loss Modulus measures the energy dissipated as heat, representing the viscous portion of the material.

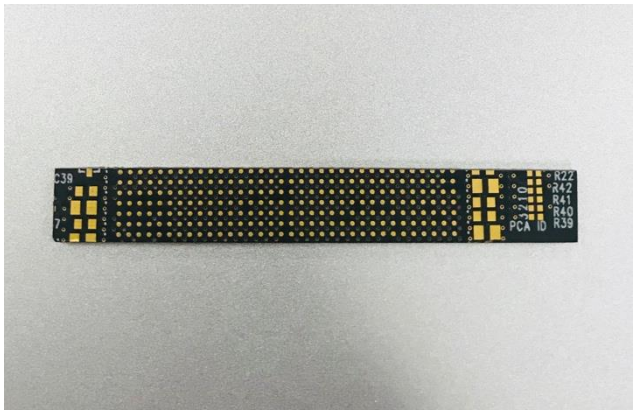

Fig :3.7 Sample used for DMA experiments

In this work, we also compare the performance for different Megtron series like Megtron GX, Megtron 2, Megtron 4, Megtron 7, and Megtron 4s. Properties of these materials are as in table 3.3 [11].

Material	CTE (ppm/^{0}C)			Young's Modulus	Poisson's Ratio
	x	y	z		
Megtron 4	14.5	14.5	35	15.9	0.2
Megtron 4s	14	14	32	15.1	0.2
Megtron 7	16	16	42	13.5	0.2
Megtron 2	15	15	34	16.7	0.2
Megtron GX	10	10	22	29	0.2

Table 3.3: Material properties for series of Megtron

Chapter 4

COMPUTATIONAL ANALYSIS

4.1 Mechanics itself is characterized by its branches being: Theoretical, Applied, Computational and Experimental. The Finite Element Methods are shelved under the computational branch. FEA are used to applications like Aerospace, automotive, nuclear, mechanical, civil. By taking a system it's always hard to analyze it and solve its complexity. If we discretize it, reduce it to its elements connected by nodes, it is possible to solve many problems. FEA helps us solve these issues in a more simplified manner than brute force practical methods. These processes provide an approximate method of solving problems.

Finite Element Modeling or Analysis is a computational approach to solve engineering and mathematical physics problems. Vibrational, Structural and thermal analysis can be done using FEA which is used by most of the companies. FEA is used to solve problems in thermal, structural, fluids, geo mechanics, electromagnetic, hydraulics, vibrations, bio medical and nuclear engineering. FEA provide us with numerous advantages. Firstly, it gives us precise geometrical constructions. Secondly, analysis can be done using various materials of a body at the same time, i.e. different materials can be assigned to one body and analysis can be done on it.

Finite element method works on the principle which divides an element into finite number of smaller elements usually with 3 to 4 nodes. Polynomial interpolation is used to find the displacement of these nodes. Equivalent system of forces at each node replaces the load or force. The governing equation is as follows,

$$[F]= [K] \{u\}$$

Where, [F] stands for force vector, [K] is Global Stiffness Matrix and {u} is the nodal displacement. The stiffness matrix depends on the material propertied like isotropic or

orthotropic and the geometry of the object. The force vector depends on the boundary conditions and the loading along with the direction of the loading applied. The nodal displacement Is obtained by mathematical methods by the software.

FEA solve problems in parts and combine the solution so as to obtain result for a complete body. This solution for structural problems helps in determining the displacement at each node and stresses in each element. Preprocessing, solution, post processing are the steps that we follow during FEA. In the Preprocessing, we create a geometric model, further elements and mesh is generated and materials properties are assigned. Secondly, in the Solution, boundary conditions and loads are applied at this step. Output and load step control is selected and the solution is obtained. In the post processing step the result is reviewed.

Few assumptions are made during FEA such as considering the PCB to be orthotropic, all materials are considered to be linear elastic except the solder, solder to be modelled as rate dependent viscoplastic material using Anand's viscoplastic model.

4.2 Geometry

Figure 4.1 shows detailed cross section of a BGA package used in this paper. BGA package has copper pad on top and bottom side of the solder ball. As seen in figure 4.1, a Silicon die is attached to the Polyimide layer with a solder mask in between them. Both sides of the board, the PCB and substrate have a layer of solder mask. The below figure is a detailed schematic diagram on a BGA package.

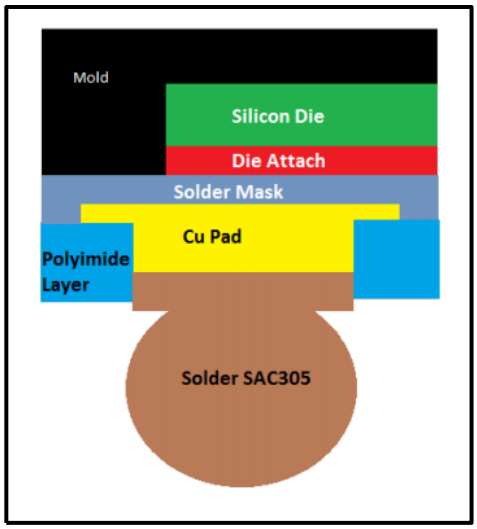

Figure 4.1: Schematic diagram for a BGA package

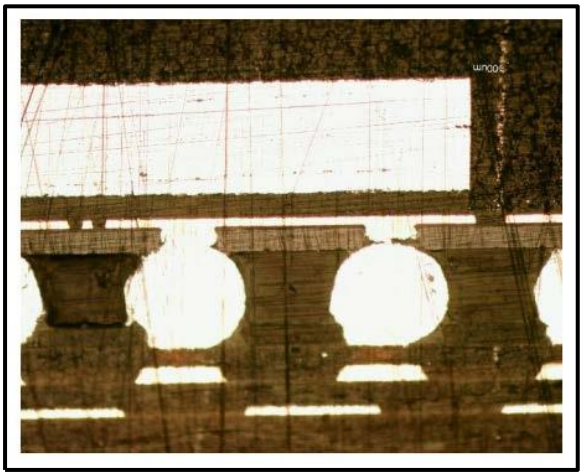

Figure 4.2: Microscopic image of a BGA package

A 3D model is developed from the X-ray image, cross sectional image of BGA and the dimensions from the drawing [2]. An octant symmetric model is used for further analysis to save the computational time as in figure 4.5. The two boards used in this paper are

Megtron 6 and FR4 where Megtron 6 consists of 18 layers (1-16-1) of copper while the FR4 board has 8 layers (1-6-1) of copper. Both the boards are approximately 2mm thick.

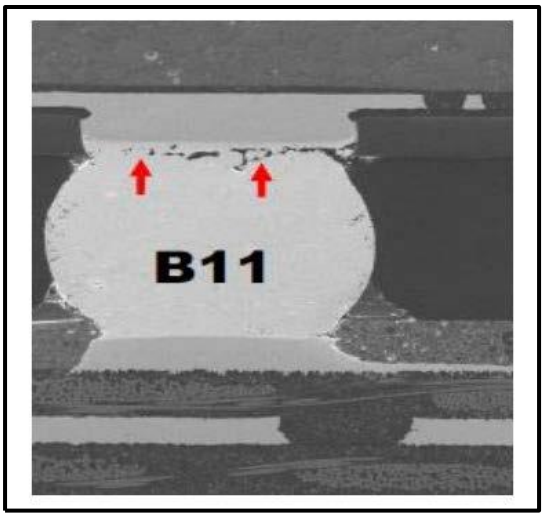

Figure 4.3: Solder ball failure towards package side

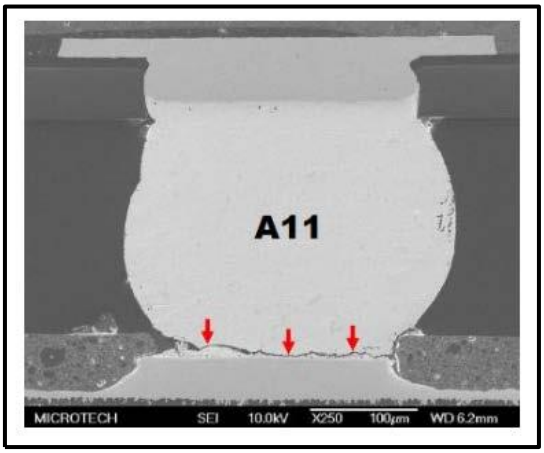

Figure 4.4: Solder ball failure towards board side

Two, 11x11 Micro star BGA package is designed with a thickness of 1mm. Solder ball reliability of this BGA package for the two boards are tested using ATC. A temperature

range of -40^{0}C to 125^{0}C with a dwell and ramp time of 15 minutes each is used for the ATC. A solder ball might fail on both the package and board side, hence it is important to perform failure analysis on these two sides. Analysis will be done depending on the results obtained in further discussions. Figure 4.3 and figure 4.4 shows failure on solder ball on the package and the board side [4].

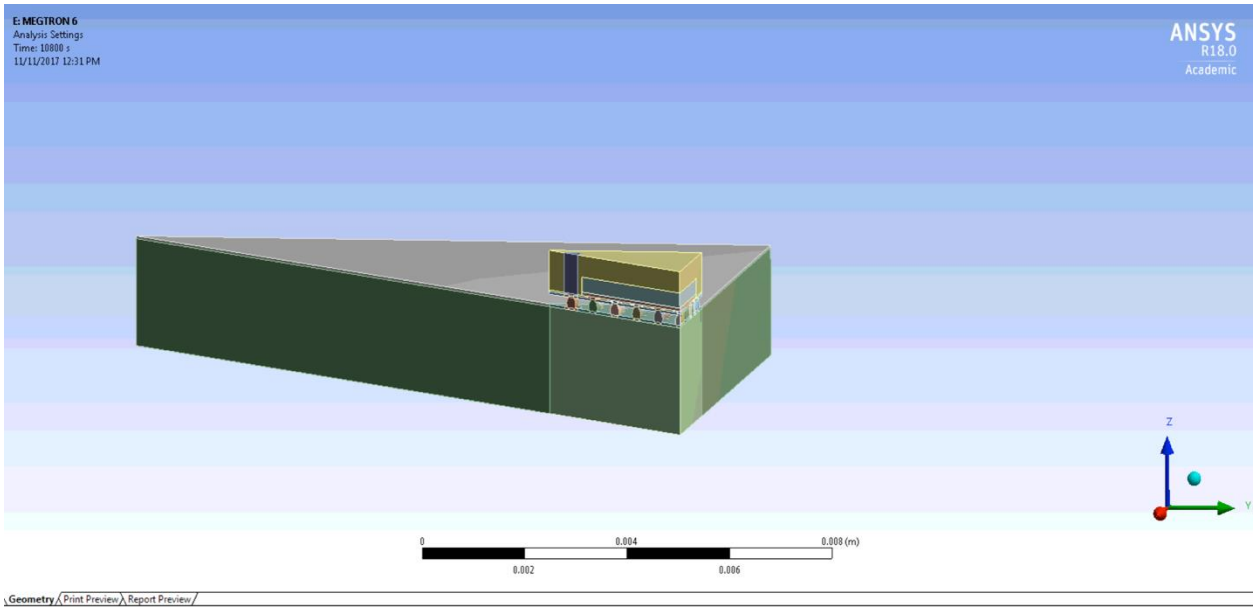

Fig: 4.5 Octant Symmetry model used for this study

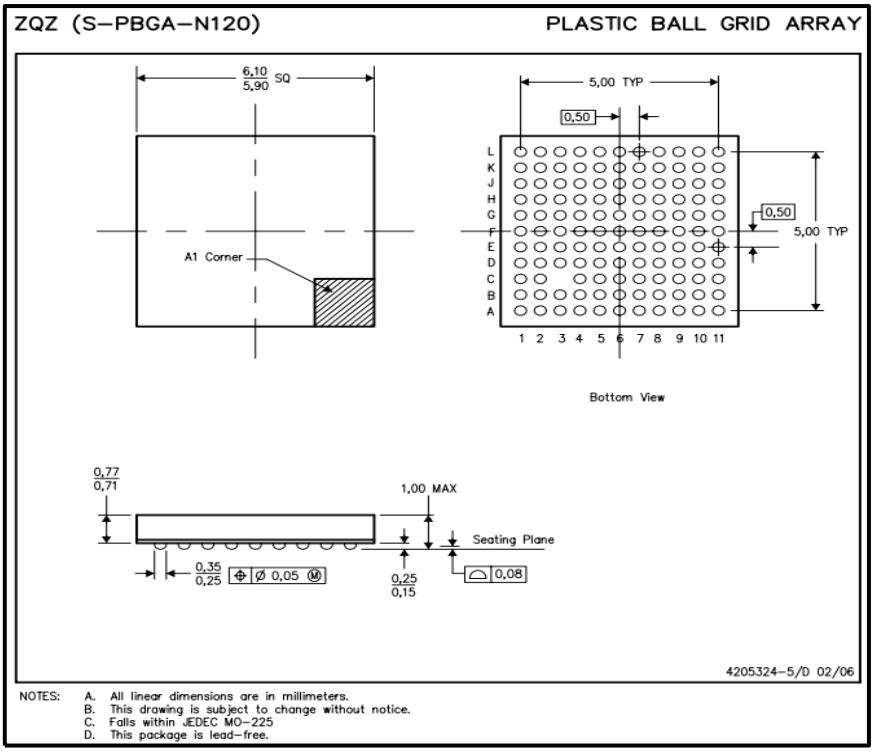

Figure 4.6: Micro star BGA drawing used to obtain unknown dimensions of BGA package

The basic configurations are obtained from the above figure 4.6.The solder ball pitch and number of solder balls is obtained from the above figures. All the dimensions are used to construct an octant symmetric model using ANSYS 18. An octant model is used so as to save the computational time.

4.3 Meshing

Hex dominant mesh is used for the solder balls. Body sizing of copper pads on the die side, substrate layer and the solder mask below the package was kept as 5E-5m. Body sizing of the solder balls (except critical solder ball), copper pads on the package side and the PCB below the package is 9E-4m. Body sizing of the critical solder ball was kept 1E-5m. Total no. of nodes and elements were 119161 and 22899 respectively.

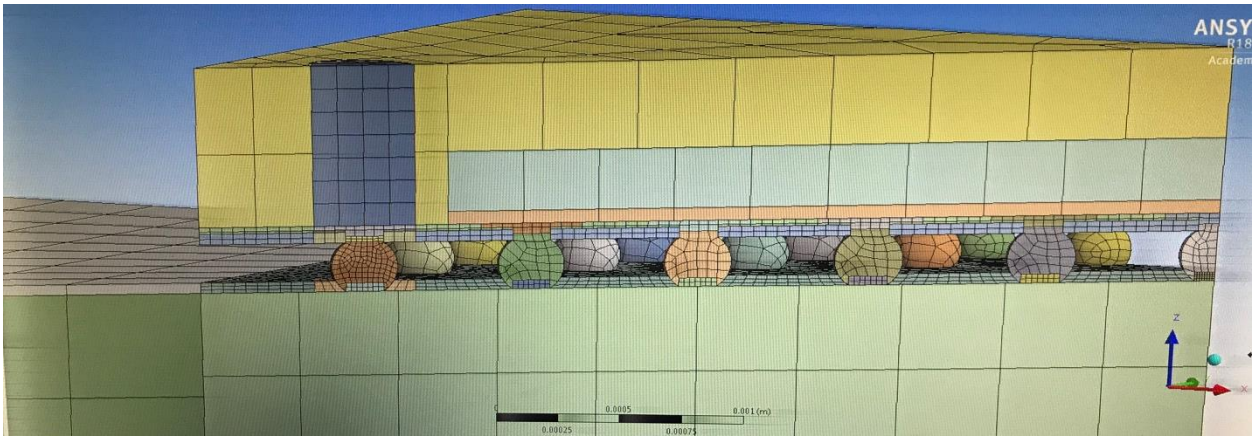

Fig: 4.7 detailed meshing

4.4 Material Properties and Boundary Condition

Symmetric boundary conditions are applied on the 2 faces towards the inside where the geometry is split. Using octant geometry does not affect the accuracy of the result. The nature of all the properties were linear elastic, except the solder joints, mold compound and the PCB. The solder joints were considered as visco-plastic and so Anand's model was used to explain the behavior of the solder joints. SAC305 is an alloy made of 96.5% tin, 3% silver and 0.5% copper. It is used as the material for solder. Anand's viscoplastic constitutive law is used to describe the inelastic part of the lead-free solder. The Anand's constants are given in the Table. The PCBs were taken as linear orthotropic in nature. As mentioned in the assumptions, Solder is modeled as rate dependent viscoplastic material which uses Anand's viscoplastic model. It takes both creep and plastic deformation into consideration to represent secondary creep of the solder. Anand's viscoplastic constitutive law best describes the inelastic behavior of lead- free solder. Anand's law consists of nine material constants A, Q, ξ, m, n, hu, a, su, ŝ.

$$\frac{d\varepsilon_p}{dt} = \text{Asinh}\left(\xi\frac{\sigma}{s}\right)^{\frac{1}{m}} \exp\left(-\frac{Q}{kT}\right)$$

$$\dot{s} = [h_0(|B|)^{\propto}\frac{B}{|B|}]\frac{d\varepsilon_p}{dt}$$

$$B = 1 - \frac{s}{s^*}$$

$$s' = \hat{s}\left[\frac{1}{A}\frac{d\varepsilon_p}{dt}\exp\left(-\frac{Q}{kT}\right)\right]^n$$

Table 3: Anand's material Constants for SAC 305 [4]

Constant	Name	Unit	Value
s_0	Initial Deformation Resistance	MPa	2.15
Q/R	Activation Energy/ Universal Gas Constant	1/K	9970
A	Pre-exponential Factor	sec^{-1}	17.994
ξ	Multiplier of Stress	Dimensionless	0.35
m	Strain Rate Sensitivity of Stress	Dimensionless	0.153
h_0	Hardening/Sof tening Constant	MPa	1525.98
$\hat{s}$	Coefficient of Deformation Resistance Saturation	MPa	2.536
n	Strain Rate Sensitivity of Saturation	Dimensionless	0.028
a	Strain Rate of Sensitivity of Hardening or Softening	Dimensionless	1.69

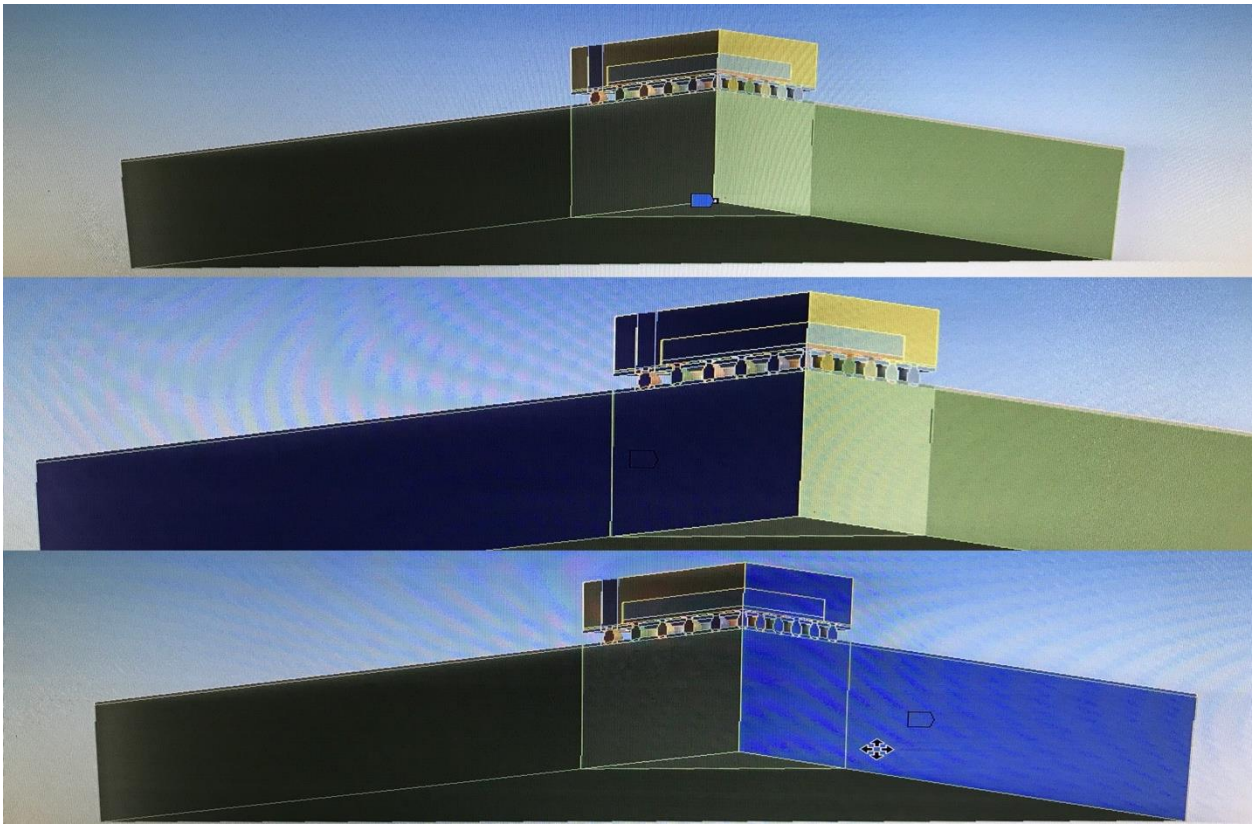

Fig: 4.8 Given Boundary Conditions

First Symmetry faces were applied on the two sides of the octant model to reduce the number of nodes and then the corner center was fixed to restrain any rigid motion.

The analysis was done in two parts. In transient thermal analysis, a convective heat transfer co-efficient is applied such that the maximum temperature in the package does not exceed $125^{o}C$. The convective heat transfer co-efficient considered for this analysis is $23W/m^2.^{o}C$. This value is chosen in such a way that it tries to match the computational analysis to experimental results. The convection is applied to outer surface of the package and PCB board.

In this study, we have assigned 3 power cycles of 0.5W/m2 in the die in the form of internal heat generation. Each cycle is 1600s, 800s being on and followed by 800s off. Total time duration was 1600 x 3 = 4800s

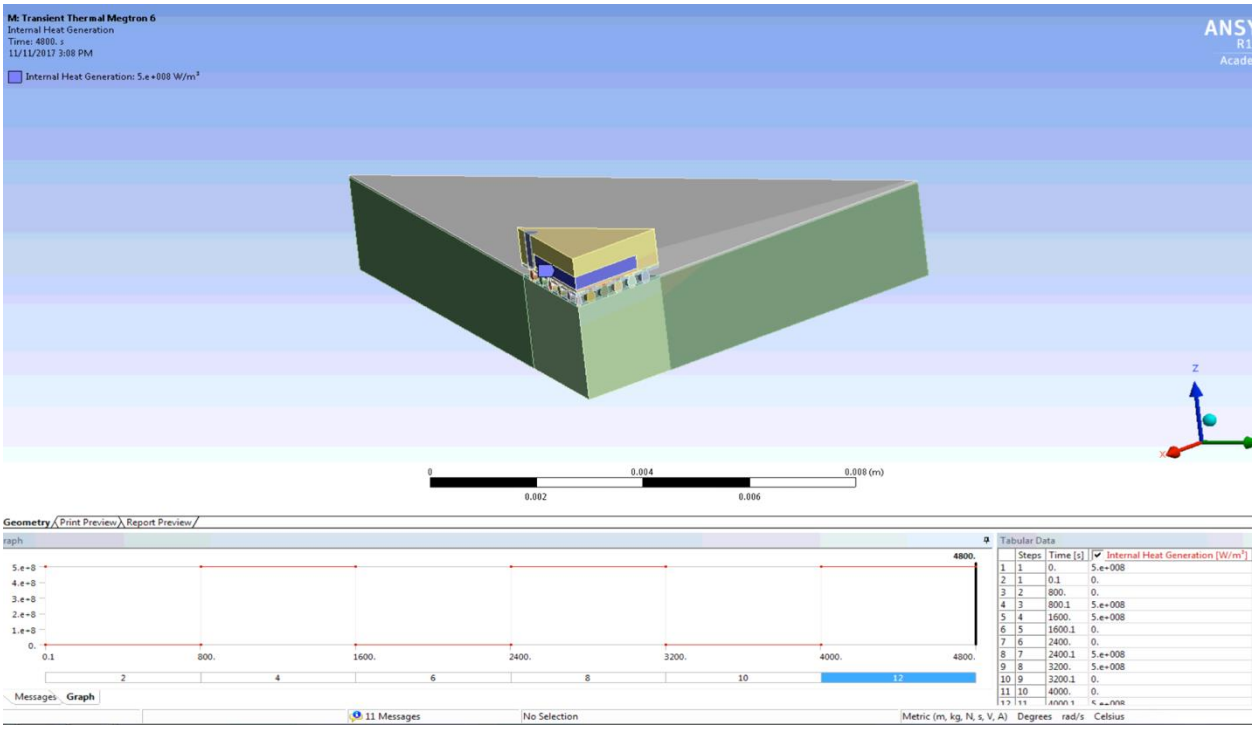

Fig :4.9 power cycle profile

(Non-Uniform Temperature Distribution)

The temperature distribution obtained from transient thermal analysis is used for static structural analysis where ATC is applied with the imported load from power cycling analysis. The die is main source of energy, so the temperature distribution shows maximum temperature near package and minimum at opposite corner of the assembly

ATC forces a uniform temperature distribution on entire package. It follows the JEDEC Standard No. 22A-10D. The test condition was from the temperature range (-40 to 125°C). The number of cycles per hour is less than 1-2. The ramp rate was taken 15 minutes and the soak time was also kept as 15 minutes.

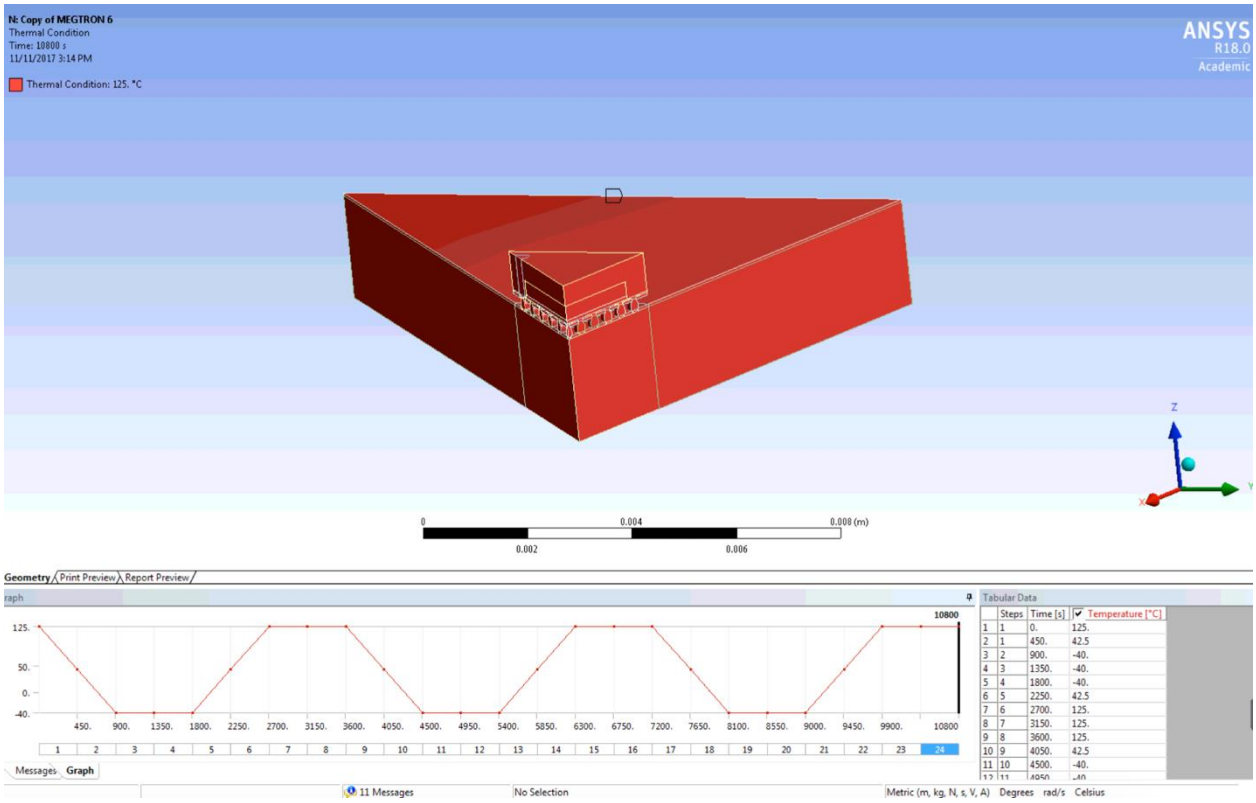

Fig :4.10 Thermal cycle profile

(Uniform Temperature Distribution)

The temperature loading profile after combining these two loads look like the profile shown in plot.

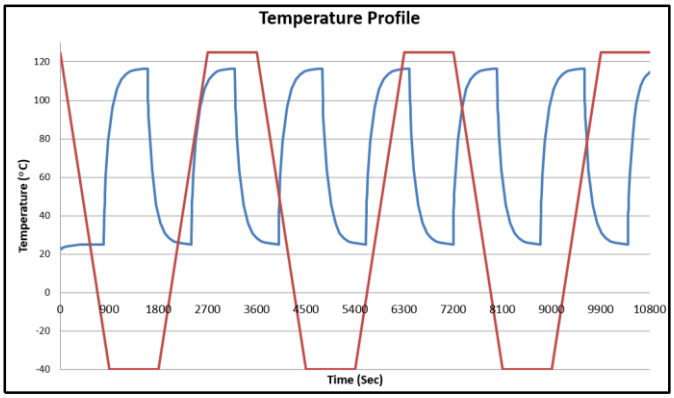

Fig :411 Combined Power cycling and thermal cycling load

Chapter 5

FATIGUE LIFE PREDICTION MODEL

5.1 Introduction

The fatigue life prediction model is used to predict life cycles to failure of the package i.e. it predicts life cycle of a package which is usually between 100 to 10,000 cycles. Due to thermo mechanical failure the solder joint fails earlier giving less life to a package. Creep strain, plastic strain range and inelastic strain energy density are the fatigue damager parameters. From the board level reliability, we can calculate the life to failure. Change in plastic work is used to predict the life to failure in this work. We use Syed's Model to predict the life cycles to failure which is as follows,

$$N_f=(674.08/\Delta W)^{(-0.9229)}$$

Where, N_f is the predicted life cycles to failure and ΔW is the change in plastic work. Using the strain energy density, Syed used a SnAgCu solder material for the life prediction of CSP and BGA packages.

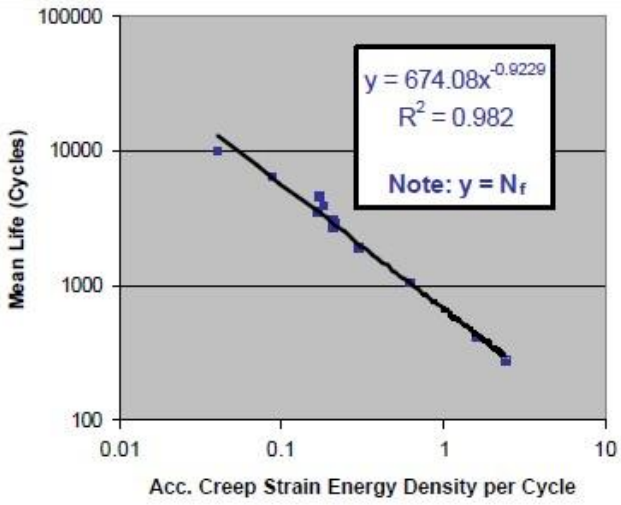

Figure 5.1: Syed's Model graph

The below figure shows a cyclic stress-strain hysteresis loop used to compare the inelastic dissipated energy that is the plastic work and the elastic strain density. This inelastic strain density is also called as the accumulated plastic work.

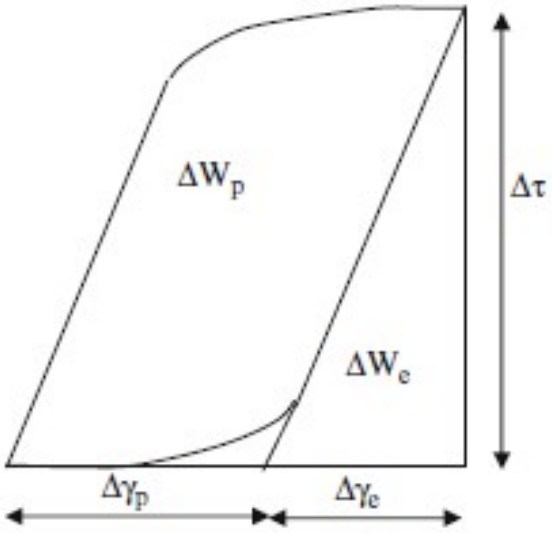

Figure 5.2: Cyclic stress-strain hysteresis loop

Chapter 6

RESULTS

A lumped model created on ANSYS 18 for computational analysis has similar meshing for Megtron and FR4 boards. Figure 4.7 shows a lumped model used for computational analysis. All the required material properties have been defined separately. Simulations for all the boards are done keeping the mesh same for all the boards.

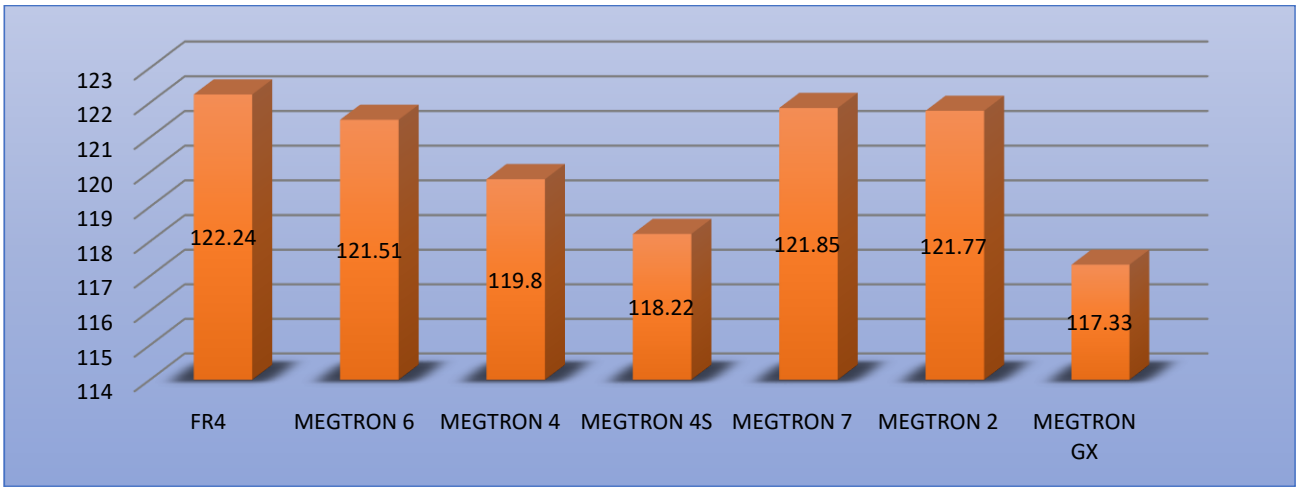

Fig: 5.3 Max temperature attained

The temperature distribution obtained from transient thermal analysis is used for static structural analysis where ATC is applied with the imported load from power cycling analysis.

After combining both thermal and power cycle it is observed that maximum stresses are at corner solder ball towards the package side. The Equivalent stress distribution comparison for Megtron series and FR4 is as shown in figure 6.1. Maximum Von Misses stresses are developed in FR4 board than any other Megtron material. The developed stresses are least in Megtron GX while as compared to Megtron 6 and FR4, Megtron 6 shows least stress. It can be seen from the figure 6.2 that maximum stresses are developed on the corner solder ball.

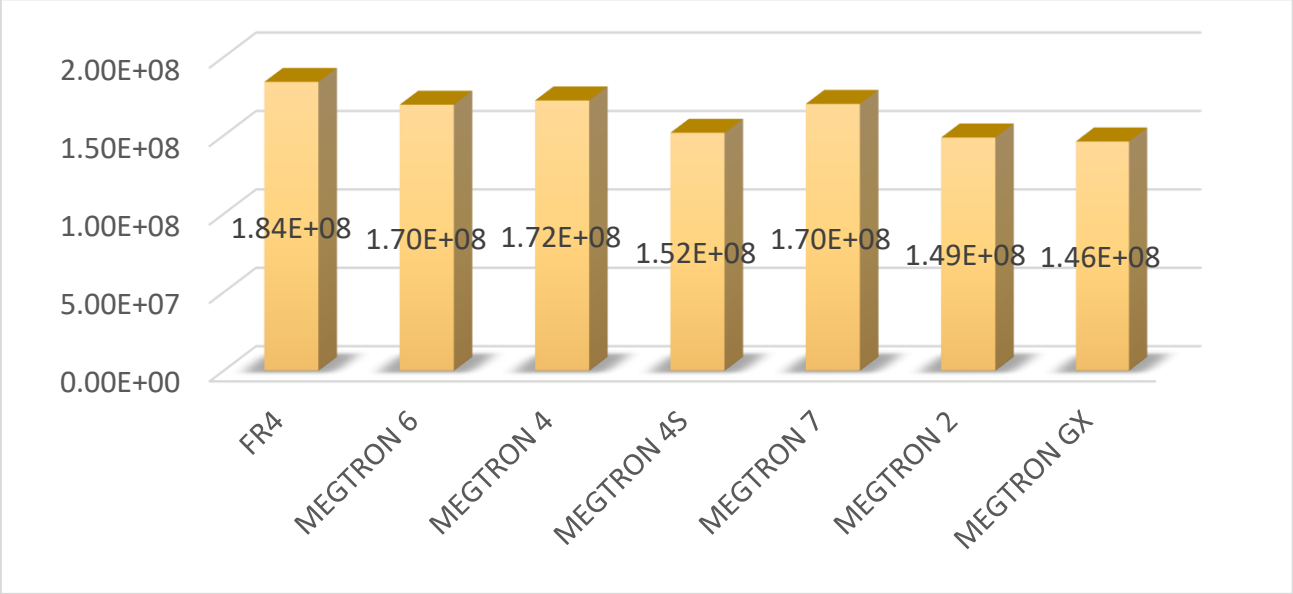

Fig: 5.4 Equivalent Stress (Pa) at the Critical Solder ball (ATC+PC)

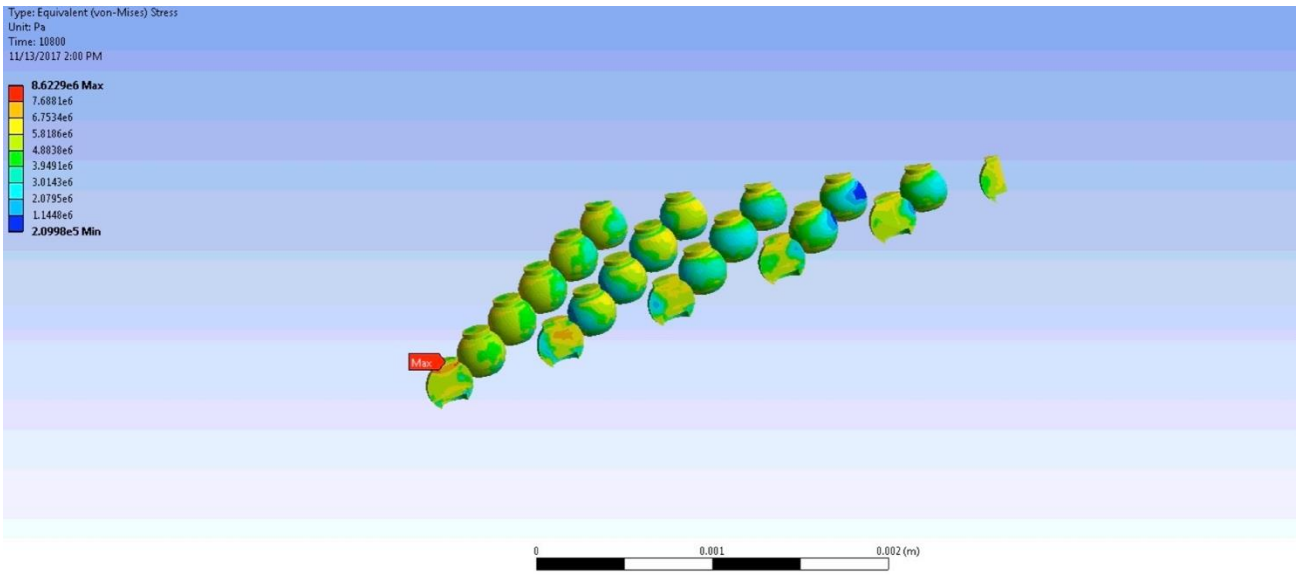

Fig: 5.5 Maximum Stress at the Corner solder ball

A similar trend is seen for the Equivalent elastic strain for these boards. The board with FR4 shows the highest strain. Strain in Megtron 6 is less than that of the FR4 board. Figure 6.4 show equivalent elastic strain graph. Equivalent stress and strain are higher in FR4 which shows that the FR4 board is stiffer than the Megtron 6 board. Maximum elastic strain is observed at the top side of the corner solder ball.

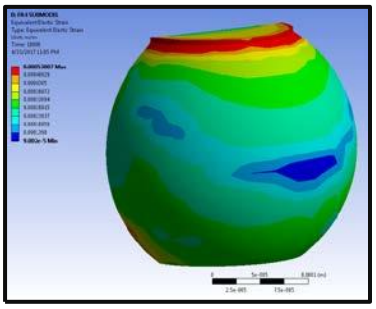

Fig: 5.6 Maximum elastic strain towards the package side

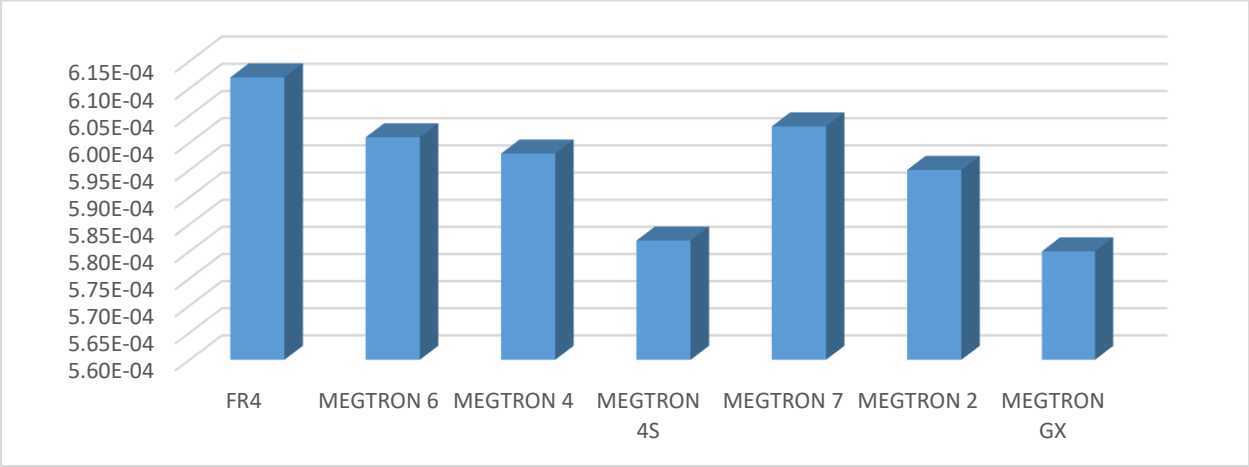

Fig: 5.6 Equivalent Elastic Strain at Critical Solder ball (ATC+PC)

The directional deformation for the boards can be seen from figure 6.5 and figure 6.6. The deformation in z axis is more than that of the x and y directions. This is because fiberglass is woven in x and y directional which restricts the expansion of the material in these directions hence the material expands in the z direction. Also, deformational in Megtron 6 is less than that of the FR4 board which is because the out of plane CTE of Megtron 6 is less than that of the FR4 board.

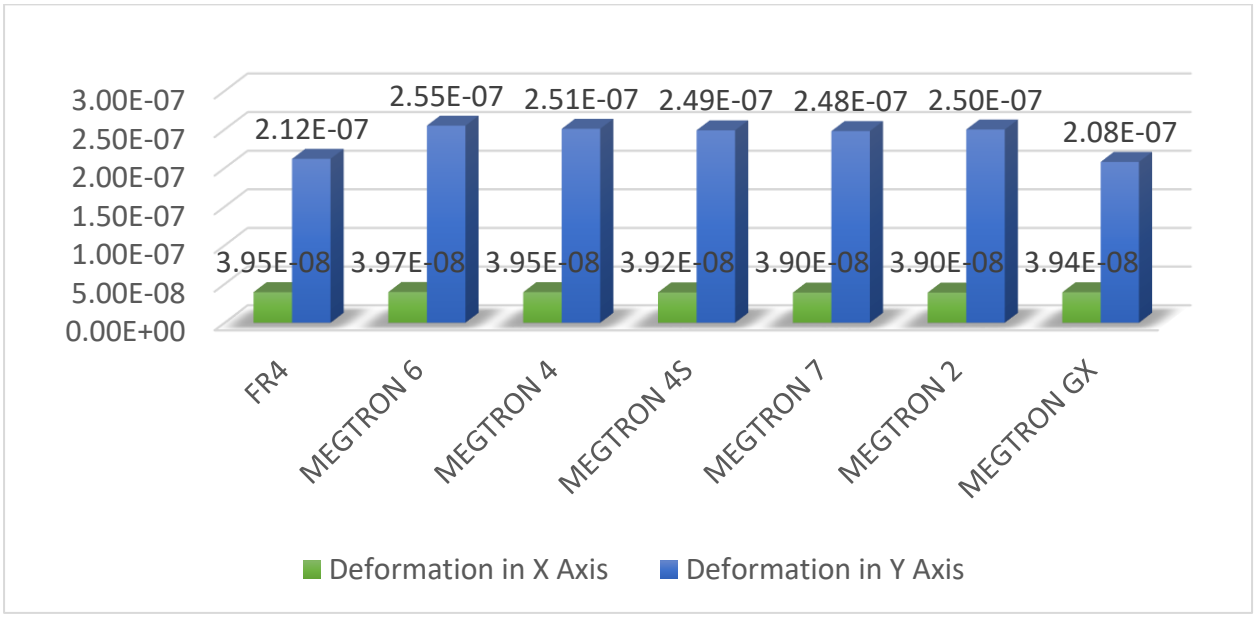

Fig: 5.7 Deformation for X and Y directions

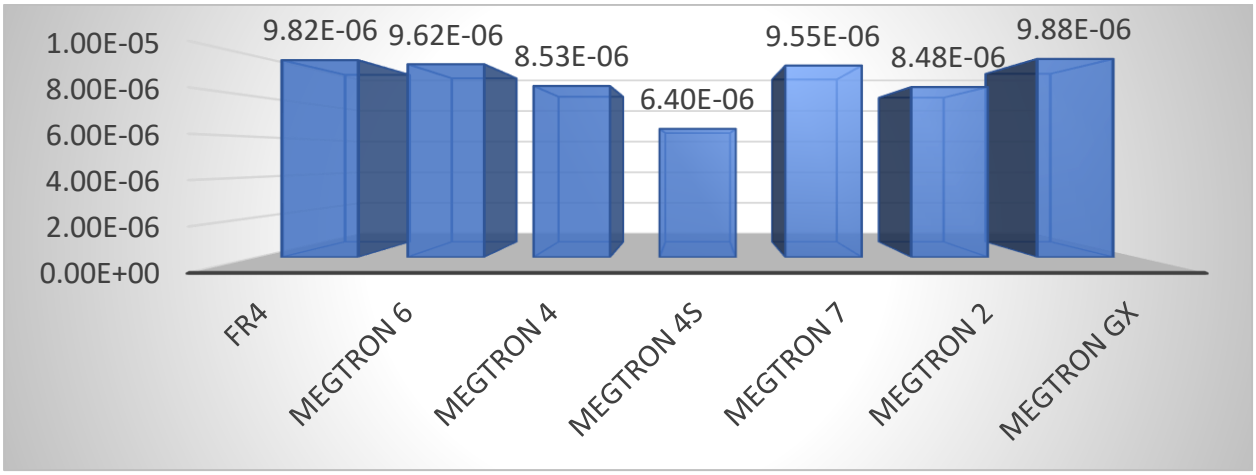

Fig: 5.8 Deformation in Z direction

It is important to calculate the change in plastic work as the solder ball is not flexible and will continue to deform it which eventually fails by cracking. We consider both sides of the solder ball to calculate the change in plastic work of the boards as the solder ball can fail on both the directions due the mismatch in CTE on both the package and board side. The change in average plastic work is calculated between the second and third cycle using Darveaux's APDL code. Figure 6.7 shows the trend in change in plastic work for the boards. The plastic work for FR-4 is almost double while compared to Megtron 6 board after combining thermal cycling with the power cycling. While Megtron 4s shows the least change in plastic work in the whole Megtron series.

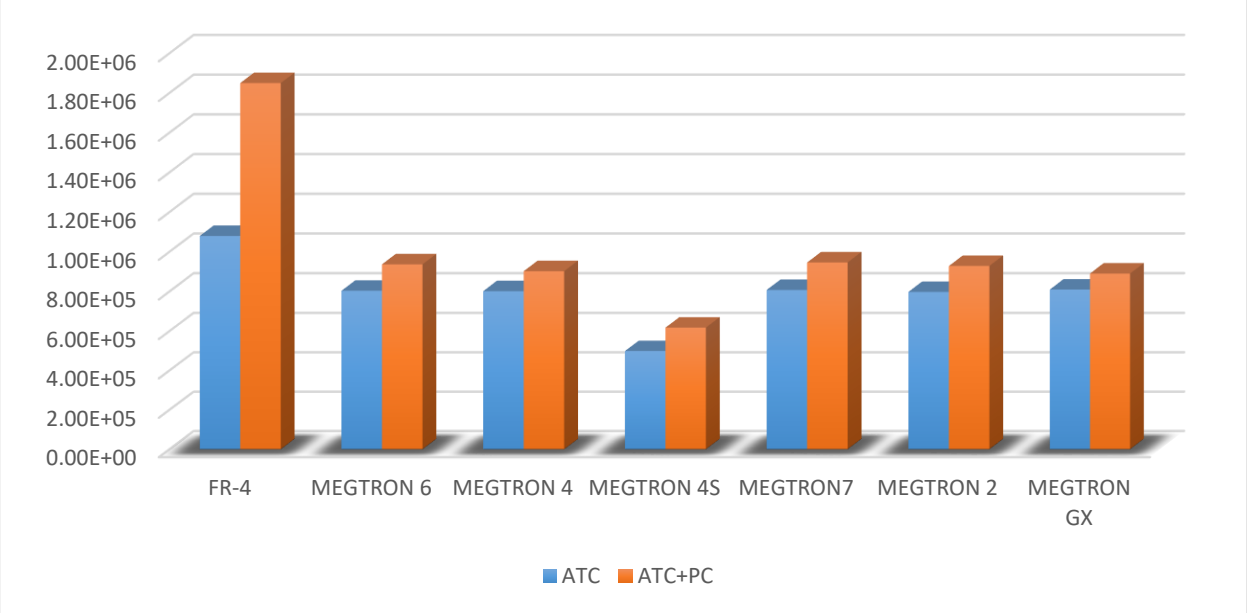

Figure: 5.9 Change in Plastic Work while subjected to ATC + PC

Figure 21 shows the change in plastic work (ΔW) for all three boards under ATC and PC+ATC. Volume average change in Plastic work between cycle 2 and 3 were calculated for both the boards using Darveaux's APDL code. [11]

Number of cycles to failure can be calculated from ΔW using Schubert et. al [8] and Che & Pang [9] correlation:

$$Nf = (A/\Delta W)^{k}$$

Where Nf is the characteristic life. A (in MPa) and k (unit less) are two empirical fatigue parameters that were used from Jie *et al.* work on chip scale packages.

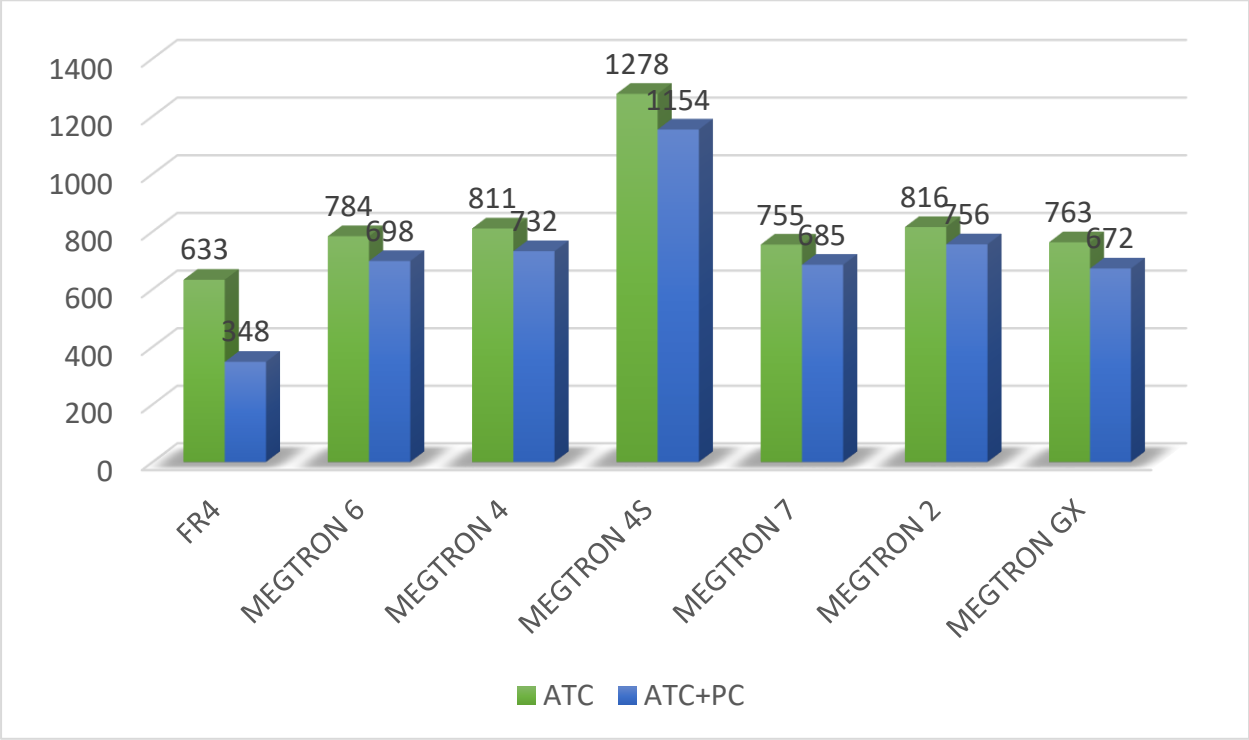

Fig: 5.10 Plot for change in plastic work Under ATC and ATC+PC

Conclusions:

The main damage mechanism that leads to failure of solder joints is the initiation and the propagation of the fatigue crack. In this work, material characterization of the boards was sucessfully done using TMA & DMA to obtain the Young's Modulus and the Co-efficient of Thermal Expansion which were used for the computational work. ANSYS 18.0 was leveraged for the equivalent stresses, equivalent elastic strains, total deformations, directional deformations, maximum temperature obtained and the solder joint fatigue analysis. The analysis includes solving a model with octant symmetry under a coupling of ATC and PC. Maximum stresses were observed on the corner solder ball towards the package. Total deformation of Megtron 6 is 11.11% less than FR-4 under ATC+PC. Megtron 4S has the least deformation in the Megtron series. Megtron GX has the least stress on the corner solder ball. Megtron 4S has the highest life to failure in the whole Megtron series under ATC+PC. Megtron 6 is found to be more durable than the conventional FR-4 by 49.74 % under the coupling of ATC and PC. Megtron series boards are proved to be more reliable and durable than the conventional FR-4 boards but very expensive (Megtron 6 costs almost more than twice when compared to FR-4).

In power cycling, the temperature distribution is non-uniform and therefore the stress distribution is also different when compared to ATC. The flexural deformation is more in Power cycling. The die is the only source of heat generation which creates more deformations in X and Y direction. ATC is conceived to generate harsher environment than PC. That's why many analyses consider only Thermal cycling for solder joint reliability assessment study but for more realistic and accurate results, PC and ATC should be applied in combined.

APPENDIX

APDL SCRIPT USED FOR STRAIN ENERGY DENSITY

! Commands inserted into this file will be executed immediately after the

ANSYS /POST1 command.

! Active UNIT system in Workbench when this object was created: Metric (m, kg, N, s, V, A)

! NOTE: Any data that requires units (such as mass) is assumed to be in the consistent solver unit system.

! See Solving Units in the help system for more information.

!APDL SCRIPT TO CALCULATE PLASTIC WORK

/post1 allsel,all

!CALC AVG PLASTIC WORK FOR CYCLE1 set,5,last,1 !LOAD STEP

cmsel,s,botsolder,elem !ELEMENT FOR VOL AVERGAING

etable,vo1table,volu pretab,vo1table

etable,vse1table,nl,plwk !PLASTIC WORK

pretab,vse1table

smult,pw1table,vo1table,vse1table

ssum

*get,splwk,ssum,,item,pw1table

*get,svolu,ssum,,item,vo1table

pw1=splwk/svolu !AVERAGE PLASTIC WORK

!CALC AVG PLASTIC WORK FOR CYCLE2

set,10,last,1 !LOAD STEP

cmsel,s,botsolder,elem

etable,vo2table,volu pretab,vo2table

```
etable,vse2table,nl,plwk !PLASTIC WORK
pretab,vse2table
smult,pw2table,vo2table,vse2table
ssum
*get,splwk,ssum,,item,pw2table
*get,svolu,ssum,,item,vo2table
pw2=splwk/svolu !AVERAGE PLASTIC WORK
!CALC DELTA AVG PLASTIC WORK
pwa=pw2-pw1
!CALC AVG PLASTIC WORK FOR CYCLE3

set,15,last,1 !LOAD STEP
cmsel,s,botsolder,elem
etable,vo3table,volu
pretab,vo3table
etable,vse3table,nl,plwk !PLASTIC WORK
pretab,vse3table smult,pw3table,vo3table,vse3table
ssum
*get,splwk,ssum,,item,pw3table
*get,svolu,ssum,,item,vo3table
pw3=splwk/svolu !AVERAGE PLASTIC WORK
!CALC DELTA AVG PLASTIC WORK
pwb=pw3-pw2
```

REFERENCES

[1] John Coonrod, “Understanding When to use FR-4 Or High Frequency Laminates”, Onboard Technology September 2011

[2] Izhar Z. Ahmed, S. B. Park, “An accurate assessment of interconnect fatigue life through power cycling” *Inter Society Conference on thermal Phenomena 2004.*

[3] Advanced Power Management Unit, Texas Instruments, SLVSAJ2–August 2010

[4] Sanjay Mahesan Revathi, “Experimental and Computational analysis on the effect of PCB layer Copper thickness and prepreg layer stiffness on solder joint reliability” University of Texas at Arlington MS-thesis, May 2015.

[5] Unique Rahangdale, “Effect of PCB thickness on solder joint reliability of Quad Flat no-lead assembly under Power Cycling and Thermal Cycling”, IEEE 2017

[6] A. Schubert, R. Dudek, E. Auerswald, A. Gollbardt, B. Michel, H. Reichl, "Fatigue Life Models for SnAgCu and SnPb Solder Joints Evaluated by Experiments and Simulation," in ECTC, 2003

[7] Lau, John H., "Effects of Build-up Printed Circuit Board Thickness on the Solder Joint Reliability of a Wafer Level Chip Scale Package (WLCSP)".

[8] Panasonic Material Properties, Panasonic

[9] Sumanth Krishnamurthy, “Experimental and Computational Board Level Reliability Assessment of Thick Board QFN Assemblies Under Power Cycling”, University of Texas at Arlington, MS-thesis, May 2016

[10] Bryan Rogers, Jeff Punch, John Jarvis, Pirkka Myllykoski, Tommi Reinikainen, “Finite Element Modelling of a BGA Package Subjected to Thermal and Power cycling”, Inter Society conference on Thermal Phenomena 2012.

[11] Jue Li, “Numerical Simulations for Reliability Assessment of Lead- Free Solder Interconnections in BGA Packages”, Aalto University Publications, Department of Electronics – Doctoral Dissertations 2011.

BIOGRAPHICAL INFORMATION

Jyotirmoy Denria received his Bachelor's in Technology (B. Tech) degree in Mechanical Engineering from West Bengal University of Technology (WBUT), Kolkata, India 2014. He pursued his Master's degree in Mechanical Engineering (MS) from the University of Texas at Arlington in fall 2017. He was an active member of EMNSPC Reliability team UTA and Surface Mount Technology Association Student Chapter at the University of Texas at Arlington. His research included experimental material characterizations of printed circuit boards performing various types of critical thermo mechanical analysis using ANSYS workbench, Spaceclaim, etc.

He was also a part of the Texas Instruments (TI) funded projects where he researched on industrial related applications. After graduation, he plans to pursue his career in the field of semiconductor industry and Electronic Packaging.